Observations of Blue Corona Discharges in Thunderclouds

Lasse Husbjerg[1], Torsten Neubert[2], Olivier Chanrion[3], Krystallia Dimitriadou[1], Dongshuai Li[1], Martin Stendel[4], Eigil Kaas[5], Nikolai Østgaard[6], and Víctor Reglero[7]

[1]National Space Institute, Technical University of Denmark (DTU Space)
[2]Department of Solar System Physics, Denmark
[3]National Space Institute (DTU Space)
[4]Danish Meteorological institute
[5]University of Copenhagen
[6]Birkeland Centre for Space Science,University of Bergen
[7]University of Valencia

November 22, 2022

Abstract

Blue electric streamer discharges in the upper reaches of thunderclouds are observed as flashes of 337.0 nm (blue) with faint or no emissions of 777.4 nm (red). Analyzing 3 years of measurements by the Atmosphere-Space Interactions Monitor (ASIM) on the International Space Station (ISS), we find that their distribution in rise time falls into two categories. One with fast rise times of 30 μs or less that are relatively unaffected by cloud scattering and emanate from within 2 km of the cloud tops, and another with longer rise times from deeper within the clouds. 46% of cells generating shallow events are associated with overshooting tops compared to 31% of cells generating deeper events. The median Convective Available Potential Energy (CAPE) of the cells is 50% higher for the shallow events and 30% higher for the deeper events than for lightning cells, suggesting the discharges are favoured by strongly convective environments.

Observations of Blue Corona Discharges in Thunderclouds

Lasse Skaaning Husbjerg[1], Torsten Neubert[1], Olivier Chanrion[1], Krystallia Dimitriadou[1], Dongshuai Li[1], Martin Stendel[2], Eigil Kaas[2,3], Nikolai Østgaard[4]and Victor Reglero[5]

[1]National Space Institute, Technical University of Denmark (DTU Space), Kgs. Lyngby, Denmark
[2]Danish Meteorological Institute, Copenhagen, Denmark
[3]University of Copenhagen, Niels Bohr Institute, København K, Denmark
[4]University of Bergen, Birkeland Centre for Space Science, Bergen, Norway
[5]University of Valencia, Image Processing Laboratory, Valencia, Spain

Key Points:

- Characterisation of blue corona discharges and their meteorological environment during 3 years of ASIM observations.
- The optical pulses of the events fall into fast ($\leq$30 μs) and slow (40 μs to 5ms) rise times, signifying different cloud depths.
- The discharges occur when CAPE is 30% - 50% larger than for lightning cells and are associated with overshooting tops 31% - 46% of the time.

Corresponding author: Lasse Skaaning Husbjerg, lhbjrg@space.dtu.dk

Abstract

Blue electric streamer discharges in the upper reaches of thunderclouds are observed as flashes of 337.0 nm (blue) with faint or no emissions of 777.4 nm (red). Analyzing 3 years of measurements by the Atmosphere-Space Interactions Monitor (ASIM) on the International Space Station (ISS), we find that their distribution in rise time falls into two categories. One with fast rise times of 30 μs or less that are relatively unaffected by cloud scattering and emanate from within ∼2 km of the cloud tops, and another with longer rise times from deeper within the clouds. 46% of cells generating shallow events are associated with overshooting tops compared to 31% of cells generating deeper events. The median Convective Available Potential Energy (CAPE) of the cells is ∼50% higher for the shallow events and ∼30% higher for the deeper events than for lightning cells, suggesting the discharges are favoured by strongly convective environments.

Plain Language Summary

Corona discharges can be seen as flashes of blue light with little or no light in a red spectral line normally emitted by lightning. They are so-called streamers and have been observed from space in the upper regions of thunderstorm clouds. In this work we present their characteristics based on 3 years of data from the Atmosphere-Space Interactions Monitor on the International Space Station. We find two categories of discharges, one is located at the very top of the clouds and the other a few kilometers inside the clouds. We find that the discharges on average are favoured by stronger convection and higher cloud tops than normal lightning.

1 Introduction

Streamers are ionisation waves in electrical discharges. A multitude of streamers may be launched, for instance, from lightning leader tips, where their optical emissions form a corona. They pre-ionize and condition the atmosphere ahead of a lightning leader, assisting its continued propagation (Raizer, 1980; Ebert et al., 2010). Flashes of light from thunderstorm clouds have been observed in $N_2$2P at 337 nm (blue) with no emission in the main lightning leader lines of OI at 777.4 nm (red), suggesting they are made of streamer breakdown. They are observed in the upper regions of clouds, with some at the very top (Kuo et al., 2009; Chang et al., 2010; Dimitriadou et al., 2022; Chanrion et al., 2017; Soler et al., 2021; Krehbiel et al., 2008; Lyons et al., 2003; N. Liu et al., 2015), and have been shown to be the associated with of Narrow Bipolar Events (NBEs) observed in VLF/LF radio signals (3-300 kHz) (F. Liu et al., 2021, 2018; Soler et al., 2020; Li et al., 2021). They are related to a wider family of discharges, which includes blue starters and blue jets that propagate from the cloud tops into the stratosphere, or beyond to the ionosphere (Wescott et al., 1995; Chanrion et al., 2017; Chou et al., 2018; P., 2008; Gordillo-Vázquez et al., 2011; Paska et al., 2012; Riousset et al., 2010; van der Velde et al., 2007). Just as NBEs occur at the onset of lightning (Rison et al., 2016), a blue corona discharge has been observed at the onset of a blue jet (Neubert et al., 2021). Consequently, they are a distinct process close to the cloud tops that is difficult to observe from the ground because the clouds interfere with the view, and the atmosphere absorbs and scatter photons. Most observations of blue discharges are from space by the ISUAL instrument (Imager of Sprites and Upper Atmospheric Lightning) on Formosat-2 (Frey et al., 2016), ASIM on the ISS (Neubert et al., 2019) and by an astronaut on the ISS (Chanrion et al., 2017). The rise time of the blue flashes range from 10μs to several ms and has been approximated with an instantaneous point source with extended rise times caused by scattering of photons in cloud particles (Soler et al., 2020; Luque et al., 2020). Therefore, the optical source is consistent with fast streamer break-down (∼10 μs) over a few kilometers, as assumed for NBEs. A study of these flashes then relates to the general problem of how lightning is triggered in clouds.

Event studies of single storms suggest that corona discharges are generated in cloud cells with strong convection (Dimitriadou et al., 2022). In order to gain a global view of their relation to storm properties, we present a statistical study of observations over 3 years by ASIM. We identify the cloud top temperature and CAPE at the time and location of each event and compare the average values of these meteorological parameters to those of a subset of normal lightning detected by ASIM.

2 The Observations

ASIM includes three photometers and two cameras. The photometers measure the second positive line of N_2 at 337 nm with a bandwidth of 5 nm (blue), part of the N_2 Lyman-Birge-Hopfield (LBH) band at 180-235 nm (UV), and a line of atomic oxygen OI at 777.4 nm with 3 nm bandwidth (red). The red line is strong in lightning leader emissions and the blue line is emitted both by leaders and streamers. The cameras measure in the blue and red bands with a spatial resolution of ∼400 m at sea level towards nadir. The instruments measure continuously during the night, but in the normal trigger mode, data is only saved when a flash is detected. In this mode, the sample rate of the photometers is 100 kHz and the frame rate of the cameras is 12 frames per second. Up to 8 frames and the corresponding photometer data are saved for each ASIM observation, with one frame before the trigger to identify the background levels. The images are cropped to the region of activity before they are queued for downlink (Chanrion et al., 2019).

Examples of the two characteristic types of blue discharges are shown in figures 1 and 2. Both occur near the coldest part of their respective cloud cell but one has a rise time of 30 μs and a duration of 1.16 ms while the other has a longer rise time of 250 μs and a duration of 2.02 ms, indicating that the fast event occurs at the cloud top while the other occurs a few kilometers below the cloud top.

The blue discharges are identified from the photometer signals. We first select the blue photometer data that contain peaks where the flux increases more than 2.5 $\mu\mathrm{Wm}^{-2}$ in 5 samples (50 μs). If more than one peak is present within ±250 samples, only the largest peak is kept. Next, we reject narrow peaks caused by energetic particle radiation, for instance, in the South Atlantic Anomaly (SAA). They are identified from the ratio of the sum of 100 samples before and 100 samples after a peak. If the ratio is less than 2, the peak is narrow and likely from energetic particles and therefore rejected. A real event will always have a tail while an energetic particle will not. For the condition of faint red emissions, we require that the ratio of the sum of 50 samples of the red and blue peaks must be less than 0.1. To be sure to reject all energetic particle events, we finally reject any remaining pulses that last less than 150 μs *and* have rise times less than 40 μs. The thresholds for the algorithms were determined empirically by testing the algorithm during times when ASIM was active in the SAA known for its high number of cosmic rays.

The events are geolocated from the measurements of the blue camera. The pixel that correspond to the maximal intensity is projected to the ground to 16 km altitude, considered an average altitude of the events. The location is cross-checked with data from the Global Lightning Detection network (GLD360) that identifies the location of electrical activity. The accuracy of projection is estimated to be better than 10 km (Neubert et al., 2021). To ensure that the cell is electrically active, GLD is checked for lightning strokes within the accuracy of the projection at ±2 minutes. If no strokes are detected, the event is discarded. It is not guaranteed that the on-board software can crop and download image data (Chanrion et al., 2019). However, all trigger events have camera meta-data containing the sums of the rows and columns from which the events can be geolocated. If the peak identified in the meta-data sums is less than 500 raw pixel digital unit counts, corresponding to approximately 4 standard deviations, the observation is discarded. If the camera image is saturated, the projection may be off by a few pixels but will remain within the 10 km uncertainty.

The Cloud Top Temperature (CTT) is from measurements by imagers on meteorological satellites, usually the channel at 10.8 μm, and accessed via the University of Wisconsin-Madison Space Science and Engineering Center (SSEC) using their software MCFetch. Depending on the location of the discharges, one of the following satellites is used: FY2G, GOES15, GOES16, MET11 or MET8. We determine the CAPE at the location of the discharges using ERA5 reanalysis data, which provides hourly estimates of various atmospheric variables in a 30 km grid. This reanalysis data is the best available estimate of the CAPE at the time of the event (Hersbach et al., 2018). We record the lowest temperature within 10 km of the event, the geolocation accuracy, the CAPE value and the tropopause temperature at the nearest grid point from the discharge in the ERA5 dataset corresponding to the CAPE within 15 km.

To understand if thunderstorms that generate blue discharges differ from those that only generate normal lightning, we have also created a lightning reference dataset that consists of 20 randomly chosen lightning observations per day during the three-year period. The procedure for geolocation and identification of the CTT and the CAPE is identical to the corona dataset.

A total of 57636 blue discharge candidates were detected, consistent with numbers quoted in (Soler et al., 2021). However, because our analysis require availability of ERA5, GLD, satellite data and that the event is strong enough geolocate, only 11625 events are included in our blue discharge dataset. The reference lightning dataset contains 9565 lightning flashes.

3 Results

The 11625 blue discharges ASIM were detected from the 1st of July 2018 to the 1st of July 2021. Their geographical distribution is shown in figure 3 where it has been smoothed by a 4×4° convolution. The discharges are found in the three main regions of high activity of normal lightning, Central America, Central Africa and South East Asia. The panels of selected regions show that the occurrences tend to be near the edge of mountains or near the coasts, particularly noticeable along the Andes mountain range. The influence of coastline and mountain topography on convection in systems that generate blue discharges will be further discussed in Section 4.

The distribution of the pulse rise times is shown in figure 4a. There appears to be two populations, one is fast pulses with rise times less than 40 μs and one is slower with longer rise times. The rise times are defined as the time between the last sample that is smaller than 10% of the peak amplitude and the first sample that is above 90% of the peak amplitude. Of the 11625 discharges, the fast population has 715 events. The distributions of the discharge duration of the two populations are shown in figure 4b. We see that the fast discharges extend to about one millisecond and the slower discharges to 2-3 milliseconds. The duration is defined as the time between the first sample above 10% of the peak amplitude and the last sample that is above 10% of the peak amplitude.

As mentioned earlier, the rise times of the optical pulses reflect how deep the discharges are in the cloud. We estimate the cloud depth L from the formula of Soler et al. (2020) as a starting point. Neglecting absorption (Luque et al., 2020) we have

$$I(t) = \frac{I_m}{\left(\frac{3}{2}\frac{t}{\tau}\right)^{\frac{3}{2}}} \exp\left(\frac{3}{2} - \frac{\tau}{t}\right) \tag{1}$$

where I_m is the maximum photon intensity, D is the diffusion coefficient for photon scattering and $\tau = \frac{L^2}{4D}$ (See supporting information S3 for the derivation). From this we can see the maximum is reached when $\frac{\tau}{t} = \frac{3}{2}$. Using the exponential of this function the 10% to 90% rise time may be approximated as $T_r \approx 0.297\tau \approx 0.0742\frac{L^2}{D}$. The cloud

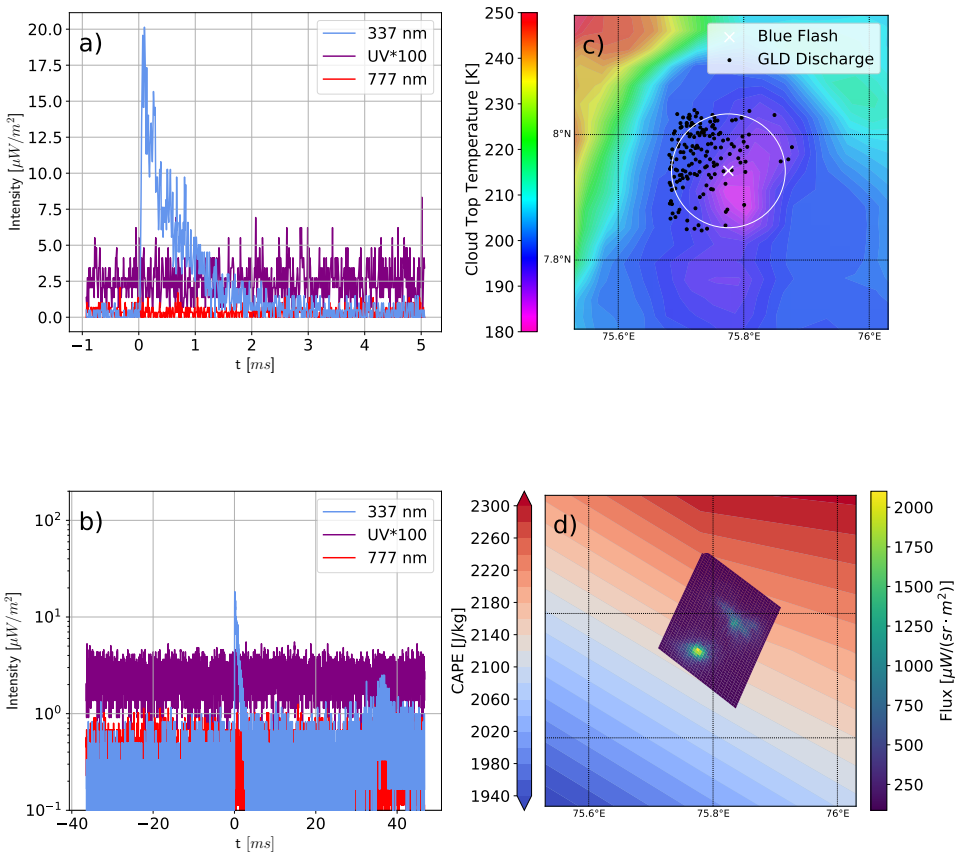

Figure 1. Fast blue discharge observed by ASIM. No present signature in the red or UV photometer. a) The photometer data for the event showing the rise time of 30 μs and a duration of 1.2 ms. b) The photometer data in log scale showing the photometer data for the full camera frame. c) Satelite data for the cloud top temperature and the event location showing that it occurs close to the coldest part of the cloud cell. The white cross determines the location of the event while the circle is the location uncertainty, black points are GLD flashes close in time to the event. d) The camera image for the event with the CAPE of the event.

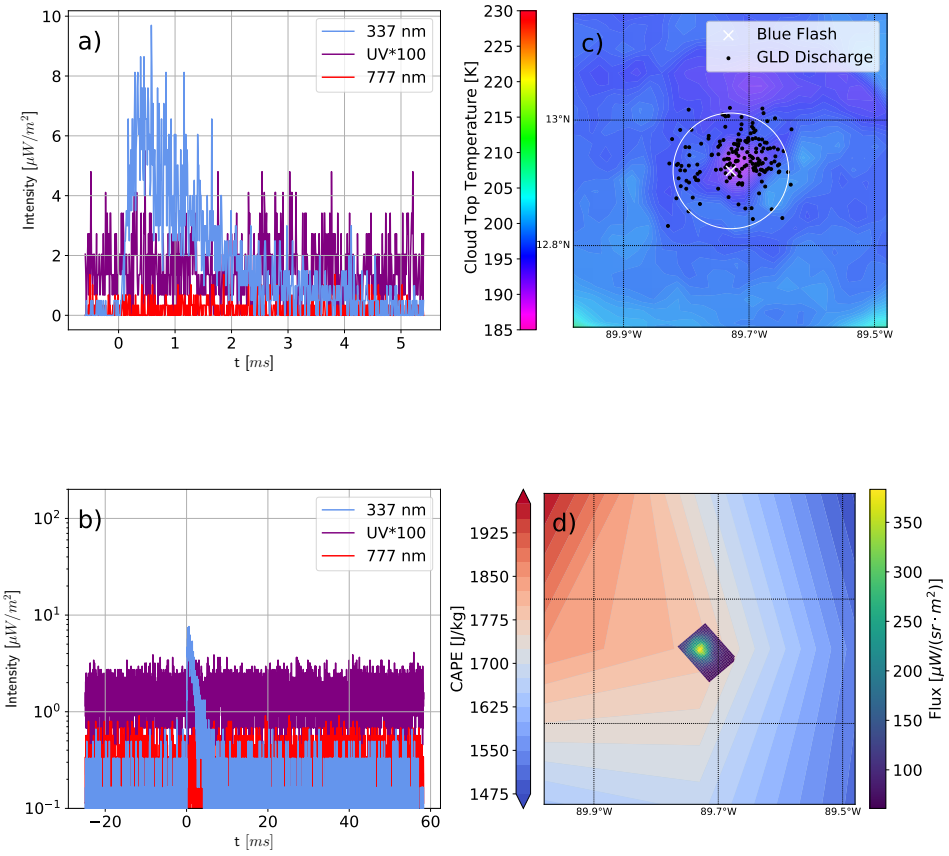

Figure 2. A slow blue discharge with a rise time of 250 μs and a duration of 2.2 ms. The cloud top temperature shows the event originating from the coldest part of the cloud and the rise time suggests an event deeper within the cloud. Panels and legend as figure 1.

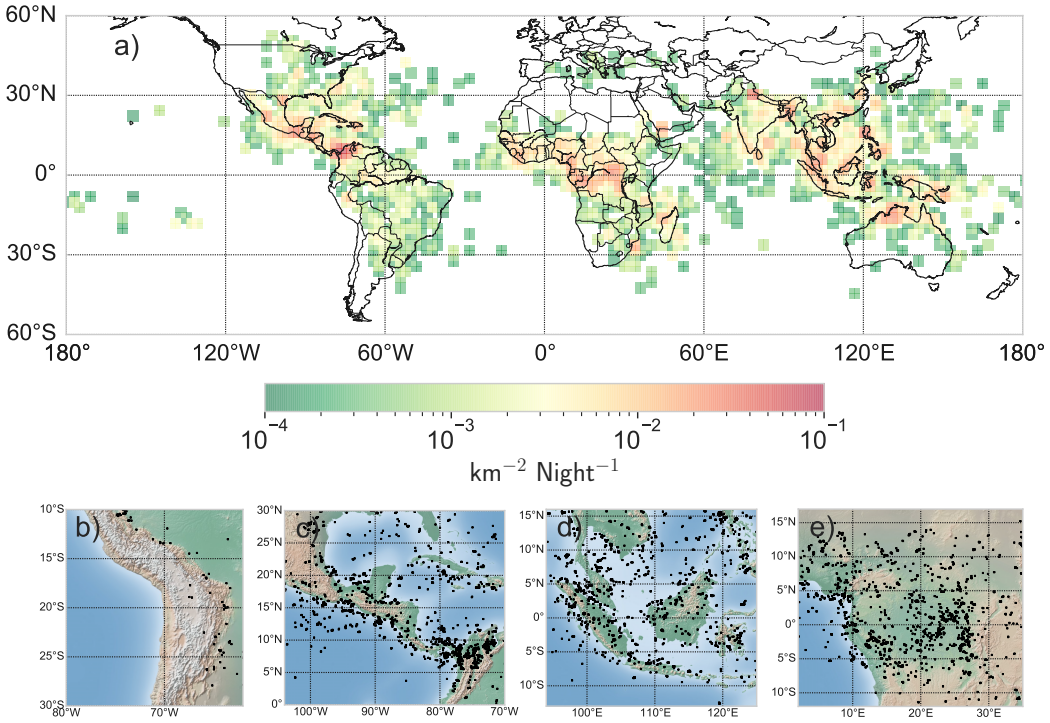

Figure 3. The global distribution of blue discharges detected by ASIM normalized by observation time with smoothing. a) The global distribution in 2° × 2° bins in the region covered by the ISS. b-e) Zoom to selected regions showing events with black markers.

depth is then

$$L = \sqrt{\frac{DT_r}{0.0742}} \tag{2}$$

with $D = 7.5{\times}10^9 \mathrm{m^2 s^{-1}}$ (Soler et al., 2020). The distribution of the cloud depths estimated from the rise times is shown in figure 4c. The fast events have an estimated cloud depth of 1-2 km while the slower events are at 2-5 km though with significant uncertainties. As we discuss in Section 4, this is consistent with altitudes of negative NBEs at the cloud tops and positive NBEs primarily at some kilometers inside the clouds (F. Liu et al., 2018; Lyu et al., 2015).

The above method is dependant on a diffusion coefficient assumed to be constant for all discharge configurations. To eliminate the variability on this parameter, which indeed depends on the ice crystal density and size distribution, we suggest an alternate method for calculating the cloud depth of the events when possible. Starting from equation 30 in Luque et al. (2020) the flux of photons without absorption is:

$$\Phi(x,y) = \frac{L}{2\pi(L^2+x^2+y^2)^{\frac{3}{2}}} \tag{3}$$

corresponding to how a pulse will look like in the ASIM camera image. Integrating this along one direction in space yields $\bar{\Phi}(x) = \frac{L}{\pi(L^2+x^2)}$. This function has a Full Width Half Maximum (FWHM) of $2L$ and allows to calculate the cloud depth of an event using the MMIA meta data which contains the sum of pixel values along the rows and columns of the MMIA camera. This method has several advantages over the previous method, in particular it is independent on the assumption on the cloud composition and its resolution is 200 meters ($\frac{1}{2}$ MMIA pixels on ground). Unfortunately it requires that there

is only one peak in the MMIA blue camera and one peak in the MMIA blue photometer. Therefore it can only be applied to about 13% of the blue discharges (1511 events with 208 fast and 1303 slow). Doing this, we see that the fast blue discharges come from about 0.8 km into the cloud while the slower discharges come from about 2 km into the cloud. Recall that the previous method used a diffusion coefficient of $7.5 \times 10^9 \mathrm{m^2 s^{-1}}$ which is based on the assumptions on the ice particle density and radius from (Soler et al., 2020). Comparing figure 4c and d we see that the diffusion coefficient might be too high and that using a value of $2.5 \times 10^9 \mathrm{m^2 s^{-1}}$ gives a better correlation between the two methods as presented in figure S2.

To determine if a relation exists between the fast blue pulses and cloud top temperature, the blue discharges have been clustered into cloud cells via density clustering. Each cluster, or cell, contains between 1 and 120 blue discharges. Every cluster is classified as containing only slow blue discharges or both fast and slow blue discharges to see if the cells differ. As shown in figure 5a, blue discharges are more likely from overshooting tops with 46% of cells which generate fast blue discharges coming from overshooting tops, compared to 31% of the cells only with slow discharges. Cells containing only lightning consists of 10% overshooting tops. Both cells generating fast blue discharges and cells generating only slow discharges are significantly more likely to be overshooting tops than regular lightning cells. There is a clear link between the both the fast and the slow blue discharges and overshooting tops, with both classifications showing that the discharges are significantly more likely to come from overshooting tops than regular lightning. Given the proportion of cells with fast discharges associated with overshooting tops the cells are likely to be linked to more severe weather systems than that of cells only with slow discharges. However, both types are also associated with more severe weather than that of lightning. The total number of events classified as cells with fast and slow discharges, and cells without fast discharges is 4495 and 7130 events, respectively.

Figure 5b shows that by clustering the blue discharge dataset as previously, cells which generate fast blue discharges have a median CAPE of 1570 $\mathrm{Jkg^{-1}}$ compared to 1280 $\mathrm{Jkg^{-1}}$ for cells generating only slow blue discharges, further indicating that stronger cells are more likely to generate fast blue discharge. For comparison, the median CAPE for regular lightning is 1000 $\mathrm{Jkg^{-1}}$. In particular the distributions differ around the low CAPE regime, wherein regular lightning is relatively common while the blue discharges are significantly rarer. A CAPE greater than 2000 $\mathrm{Jkg^{-1}}$ usually indicates deep convection. Cells generating fast blue discharges have 25% occur in the region of deep convection. For cells generating only slow blue discharges it is 17% while for regular lightning, only 10% of the events have a CAPE greater than 2000 $\mathrm{Jkg^{-1}}$. Therefore, there is a strong link between deep convection and the generation of blue discharge events. All parameters presented here suggest that both fast and slow blue discharges are favoured by more severe weather than that required for lightning strokes.

4 Discussions and Conclusion

The catalogue presented here is the first of its kind to compare blue discharge cell systems with their local meteorological parameters. To further the understanding of how lightning is triggered in clouds, it is important to determine if these systems are significantly different from those generating only regular lightning.

The geographical distribution of events show clear correlations between regions with higher average lightning activity and blue discharge generation. Furthermore, the blue discharges are usually generated near the coasts or near the ridges of mountains except in the central Africa region. There blue discharge events occur relatively evenly everywhere likely due to the extremely high atmospheric instability. Coastal regions are areas of significant atmospheric instability and it has been shown that the exact topography of the land-sea contrast can have large effects on the convection initiation in those

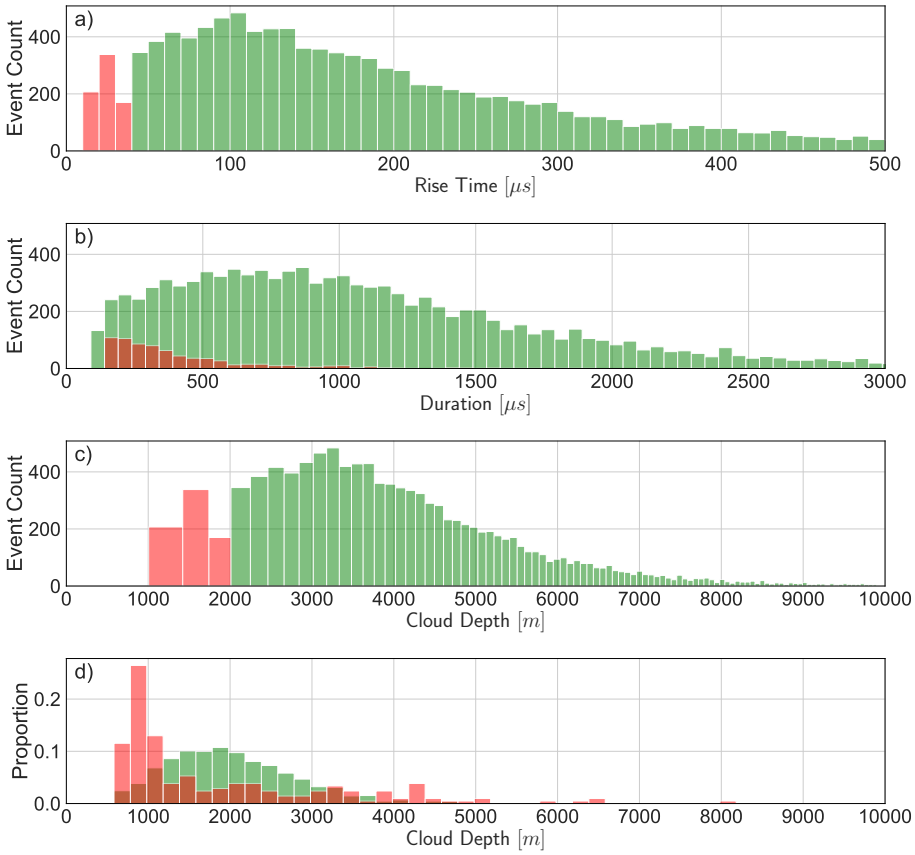

Figure 4. Rise time and duration of all blue discharge observed in the 3 year (July 1st 2018 to July 1st 2021) interval with binsizes of 10 μs and 50 μs, respectively. Red coloured bins indicate a fast blue discharge with rise time less than 40 μs and green a rise time greater than 40 μs. a) The rise times for the blue discharges, with medians for the two distributions at 20 μs and 170 μs. b) Distribution of durations of blue discharges with a median of 1 ms. c) The calculated cloud depth of the event sources given the detected rise times, the median of the two peaks have cloud depth of 1.4 km and 3.2 km respectively. d) The cloud depth calculated from the camera image using a subset of the available events showing a peak for the fast events at 0.8 km, binsize is 200 m. The two peaks indicate two separate types of events, one at cloud tops close to the tropopause with a fast rise time and another originating deeper into the cloud system with a correspondingly lower rise time.

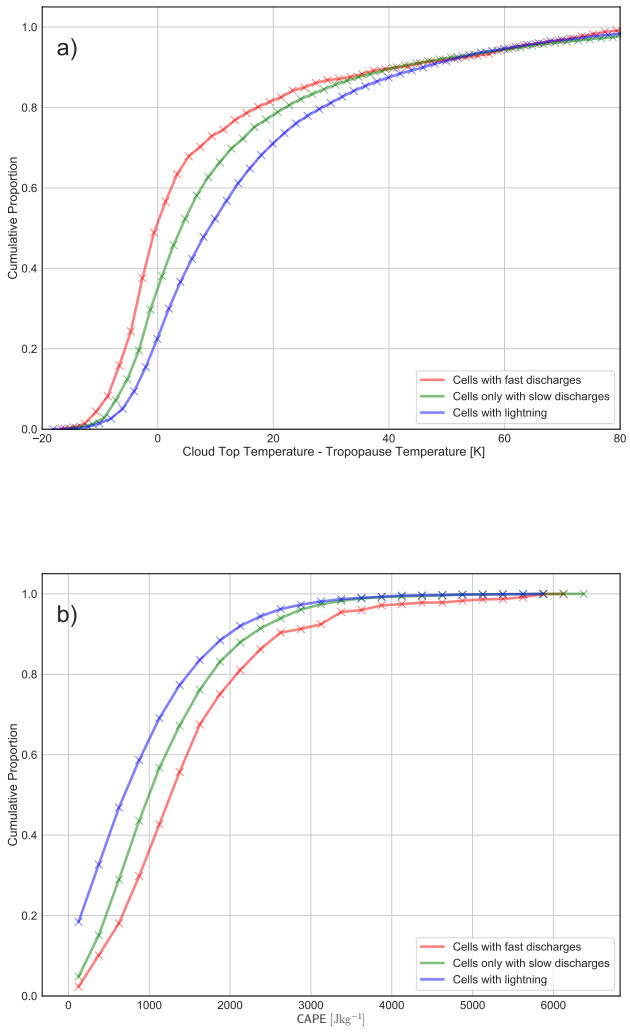

Figure 5. Cumulative distribution of CAPE and CTT difference of the blue discharges compared to regular lightning detected by MMIA normalized by total number of events. Individual blue discharge observations are clustered into cells via density clustering and considered coming from a cell generating fast blue discharges if there is at least one fast blue discharge in its cell. Of the cells generating fast blue discharges, 46% are overshooting tops, compared to 31% of the cells only with slow discharges. Cells containing only lightning consists of 10% overshooting tops. About 25% of cells with fast discharges occur during deep convection (CAPE greater than 2000 Jkg^{-1}), compared to 17% of cells only with slow discharges and 10% of lightning cells.

regions (Bai et al., 2020). It is therefore likely that the relatively higher instability and propensity for convection is the cause of the abundance of blue discharges observed near coasts. While the link between mountains and convection is less well characterized, it is known that the topography of mountain ranges have an important role in understanding the properties of local convection (Kirshbaum, 2011; Serafin & Zardi, 2010). Furthermore the Andes mountain range is known to have a significant effect on the deep convective processes of South America (Insel et al., 2010). Both the fast and slow blue discharges appear to require the deep convective processes which are found mainly in areas with strong contrasting topography such as mountain ranges and coastlines as well as a moist environment.

Studies show that blue discharges are linked to NBEs which are known to occur at different cloud depths depending on the polarity of the NBE as is seen in this separate distribution of rise times of the blue discharges (F. Liu et al., 2018). A subset of blue discharges are likely a result of NBE events with a significant part of the shallow events coming from negative NBEs. The strong separation between the cloud depths as determined by the rise time distribution indicate that they are two separate types of events. The first peak in the rise times is associated with negative NBEs and it is likely that the second peak contains many positive NBEs. This is further suggested by the large proportion of fast and slow blue discharges associated with overshooting tops. NBEs are often associated with overshooting tops and severe weather which is supported by the data presented here (F. Liu et al., 2021; Monette et al., 2012). It is possible that the separated peaks in the rise times are indirectly measuring the charge regions of the cloud, though with significant uncertainty on the size of the region. In that case, the rise time distribution of events may be a useful way to probe the charge layers of a given thunderstorm.

We have presented the first dataset of blue discharges which compares important meteorological parameters for these events with systems generating only regular lightning. By inspecting the rise time distribution of the events, we see two separate event types characterized by the cloud depth of their source, strongly indicating a link between blue discharges and NBEs. Understanding how the generating systems differ from systems which produce only lightning is an important step in expanding the understanding of the deeper mechanisms which cause the blue discharges and therefore how lightning triggers in clouds.

Acknowledgments

The authors thank Dr. Francisco J. Gordillo-Vazquez for fruitful discussions during the preparation of the paper, VAISALA for the GLD360 lightning data, ECMWF for the ERA5 reanalysis data and SSEC for making the satellite data available. ERA5 data was downloaded from the Copernicus Climate Change Service (C3S) Climate Data Store (Hersbach et al., 2018). The results contain modified Copernicus Climate Change Service information 2020. Neither the European Commission nor ECMWF is responsible for any use that may be made of the Copernicus information or data it contains. ASIM is a mission of the European Space Agency (ESA) and is funded by ESA and by national grants of Denmark, Norway and Spain. The ASIM Science Data Centre is supported by ESA PRODEX contracts C 4000115884 (DTU) and 4000123438 (Bergen).

Data Availability Statement

Data supporting this research are available at `https://asdc.space.dtu.dk`, with agreement from the ASIM Facility Science Team (FST), and are not accessible to the public or research community. Interested researchers should submit a research proposal to the FST through asdc@space.dtu.dk. GLD360 data may be obtained through agreement with VAISALA. ERA5 reanalysis data download and instructions are available at `https://www.ecmwf.int/en/forecasts/datasets/reanalysis-datasets/era5` for registered users. All satellite images used can be accessed using MCFetch for registered users, with instructions available at `https://mcfetch.ssec.wisc.edu/`.

References

Bai, L., Chen, G., & Huang, L. (2020). Convection Initiation in Monsoon Coastal Areas (South China). *Geophysical Research Letters*, *47*(11), e2020GL087035. doi: https://doi.org/10.1029/2020GL087035

Chang, S. C., et al. (2010). ISUAL far-ultraviolet events, elves, and lightning current. *Journal of Geophysical Research: Space Physics*, *115*(A7). doi: https://doi.org/10.1029/2009JA014861

Chanrion, O., Neubert, T., Mogensen, A., Yair, Y., Stendel, M., R.Singh, & Singh, D. (2017). Profuse activity of blue electrical discharges at the tops of thunderstorms. *Geophysical Research Letters*, *44*(1), 496–503. doi: https://doi.org/10.1002/2016GL071311

Chanrion, O., Neubert, T., Rasmussen, I. L., et al. (2019). The Modular Multispectral Imaging Array (MMIA) of the ASIM Payload on the International Space Station. *Space Science Review*, *215*(28). doi: https://doi.org/10.1007/s11214-019-0593-y

Chou, J. K., Hsu, R. R., Su, H. T., Chen, A. B. C., Kuo, C. L., Huang, S. M., & Wu, Y. J. (2018). ISUAL-Observed Blue Luminous Events: The Associated Sferics. *Journal of Geophysical Research: Space Physics*, *123*(4), 3063–3077. doi: https://doi.org/10.1002/2017JA024793

Dimitriadou, K., et al. (2022). Analysis of blue corona discharges at the top of tropical thunderstorm clouds in different phases of convection. *Geophysical Research Letters*, 49. doi: https://doi.org/10.1029/2021GL095879

Ebert, U., Nijdam, S., Li, C., Luque, A., Briels, T., & vand Veldhuizen, E. (2010). Review of recent results on streamer discharges and discussion of their relevance for sprites and lightning. *Journal of Geophysical Research: Space Physics*. doi: 10.1029/2009JA014867

Frey, H. U., et al. (2016). The Imager for Sprites and Upper Atmospheric Lightning (ISUAL). *Journal of Geophysical Research: Space Physics*, *121*(8), 8134-8145. doi: https://doi.org/10.1002/2016JA022616

Gordillo-Vázquez, F. J., Luque, A., & Simek, M. (2011). Near infrared and ultraviolet spectra of TLEs. *Journal of Geophysical Research: Space Physics*. doi: doi:

10.1029/2012JA017516

Hersbach, H., et al. (2018). *ERA5 hourly data on single levels from 1979 to present. Copernicus Climate Change Service (C3S) Climate Data Store (CDS).* doi: 10.24381/cds.adbb2d47

Insel, N., Poulsen, C. J., & Ehlers, T. A. (2010). Influence of the andes mountains on south american moisture transport, convection, and precipitation. *Climate Dynamics*, *35*, 1477 - 1492. doi: 10.1007/s00382-009-0637-1

Kirshbaum, D. J. (2011). Cloud-resolving simulations of deep convection over a heated mountain. *Journal of the Atmospheric Sciences*, *68*(2), 361 - 378. doi: 10.1175/2010JAS3642.1

Krehbiel, P. R., Riousset, J. A., Pasko, V. P., Thomas, R. J., Rison, W., Stanley, M. A., & Edens, H. E. (2008). Upward electrical discharges from thunderstorms. *Nature Geoscience*, *1*(4), 233–237. doi: 10.1038/ngeo162

Kuo, C.-L., et al. (2009). Discharge processes, electric field, and electron energy in ISUAL-recorded gigantic jets. *Journal of Geophysical Research: Space Physics*, *114*(A4). doi: https://doi.org/10.1029/2008JA013791

Li, D., Luque, A., Gordillo-Vázquez, F. J., Liu, F., Lu, G., Neubert, T., & Reglero, V. (2021). Blue Flashes as Counterparts to Narrow Bipolar Events: the Optical Signal of Shallow In-Cloud Discharges. *Journal of Geophysical Research: Atmospheres*, 1–13. doi: 10.1029/2021jd035013

Liu, F., et al. (2018). Observations of Blue Discharges Associated With Negative Narrow Bipolar Events in Active Deep Convection. *Geophysical Research Letters*, *45*(6), 2842-2851. doi: https://doi.org/10.1002/2017GL076207

Liu, F., et al. (2021). Optical emissions associated with narrow bipolar events from thunderstorm clouds penetrating into the stratosphere. *Nature Communications*, *12*. doi: https://doi.org/10.1038/s41467-021-26914-4

Liu, F., Zhu, B., Lu, G., & Ma, M. (2021). Outbreak of Negative Narrow Bipolar Events in Two Mid-Latitude Thunderstorms Featuring Overshooting Tops. *Remote Sensing*, *13*(24). doi: 10.3390/rs13245130

Liu, N., McHarg, M. G., & Stenbaek-Nielsen, H. C. (2015). High-altitude electrical discharges associated with thunderstorms and lightning. *Journal of Atmospheric and Solar-Terrestrial Physics*, *13*, 98–118. doi: 10.1016/j.jastp.2015.05.013

Luque, A., et al. (2020). Modeling lightning observations from space-based platforms (CloudScat.jl 1.0). *Geoscientific Model Development*, *13*(11), 5549–5566. doi: 10.5194/gmd-13-5549-2020

Lyons, W. A., Nelson, T. E., Armstrong, R. A., Pasko, V. P., & Stanley, M. A. (2003). Upward electrical discharges from thunderstorm tops. *Bulletin of the American Meteorological Society*, *84*(4), 445–454. doi: 10.1175/BAMS-84-4-445

Lyu, F., Cummer, S. A., & McTague, L. (2015). Insights into high peak current in-cloud lightning events during thunderstorms. *Geophysical Research Letters*, *42*(16), 6836-6843. doi: https://doi.org/10.1002/2015GL065047

Monette, S. A., Velden, C. S., Griffin, K. S., & Rozoff, C. M. (2012). Examining Trends in Satellite-Detected Tropical Overshooting Tops as a Potential Predictor of Tropical Cyclone Rapid Intensification. *Journal of Applied Meteorology and Climatology*, 1917–1930. doi: https://doi.org/10.1175/JAMC-D-11-0230.1

Neubert, T., et al. (2021). Observation of the onset of a blue jet into the stratosphere. *Nature*, *589*, 375–379. doi: 10.1038/s41586-020-03122-6

Neubert, T., Østgaard, N., Reglero, V., Blanc, E., Chanrion, O., Oxborrow, C. A., & Bhanderi, D. D. (2019). The ASIM Mission on the International Space Station. *Space Science Reviews*. doi: 10.1007/s11214-019-0592-z

P., P. V. (2008). Blue jets and gigantic jets: Transient luminous events between thunderstorm tops and the lower ionosphere. *Plasma Physics and Controlled*

Fusion, *50*(12). doi: 10.1088/0741-3335/50/12/124050

Paska, V. P., Yair, Y., & Kuo, C. L. (2012). Lightning related transient luminous events at high altitude in the earth's atmosphere: Phenomenology, mechanisms and effects. *Space Science Reviews*. doi: 10.1007/s11214-011-9813-9422

Raizer, P. (1980). *Fundamentals of the contemporary physics of gas discharge processes* .

Riousset, J. A., Paska, V. P., Krehbiel, P. R., Kison, W., & Stanley, M. A. (2010). Modeling of thundercloud screening charges: Implications for blue and gigantic jet. *Journal of Geophysical Research: Space Physics*. doi: 10.1029/2009ja014286

Rison, W., Krehbiel, P. R., Stock, M. G., Edens, H. E., Shao, X. M., Thomas, R. J., & Zhang, Y. (2016). Observations of narrow bipolar events reveal how lightning is initiated in thunderstorms. *Nature Communications*. doi: 10.1038/ncomms10721

Serafin, S., & Zardi, D. (2010). Daytime heat transfer processes related to slope flows and turbulent convection in an idealized mountain valley. *Journal of the Atmospheric Sciences*, *67*(11), 3739 - 3756. doi: 10.1175/2010JAS3428.1

Soler, S., et al. (2020). Blue Optical Observations of Narrow Bipolar Events by ASIM Suggest Corona Streamer Activity in Thunderstorms. *JGR Atmospheres*. doi: 10.1029/2020JD032708

Soler, S., et al. (2021). Global Frequency and Geographical Distribution of Nighttime Streamer Corona Discharges (BLUEs) in Thunderclouds. *Geophysical Research Letters*, *48*(18), e2021GL094657. (e2021GL094657 2021GL094657) doi: https://doi.org/10.1029/2021GL094657

van der Velde, O. A., Lyons, W. A., Nelson, T. E., Cummer, A. S., Li, K., & Bunnel. (2007). Analysis of the first gigantic jet recorded over continental North America. *Journal of Geophysical Research Atmospheres*. doi: 10.1029/2007JD008575

Wescott, E. M., Sentman, D., Osborne, D., Hampton, D., & Heavner, M. (1995). Preliminary results from the Sprites94 Aircraft Campaign: 2. Blue jets. *Geophysical Research Letters*, *22*(10), 1209–1212. doi: 10.1029/95GL00582

Supporting Information for "Characteristics of Blue Corona Discharges observed by ASIM"

Lasse Skaaning Husbjerg[1], Torsten Neubert[1], Olivier Chanrion[1], Krystallia Dimitriadou[1], Dongshuai Li[1], Martin Stendel[2], Eigil Kaas[2,3], Nikolai Ostgaard[4], and Reglero Victor[5]

[1]National Space Institute, Technical University of Denmark (DTU Space), Kgs. Lyngby, Denmark

[2]Danish Meteorological Institute, Copenhagen, Denmark

[3]University of Copenhagen, Nils Bohr Institute, København K, Denmark

[4]University of Bergen, Birkeland Centre for Space Science, Bergen, Norway

[5]University of Valencia, Image Processing Laboratory, Valencia, Spain

Contents of this file

1. Text S1 to S3

2. Figure S1 to S2

Introduction The supplementary information describes the process of calculating rise times and durations for the blue events, how to correct for satellite parallax and the derivation of the cloud depth coefficient. Additionally, there is a figure of the geographical distribution of events without smoothing applied and a figure with the better estimate for the cloud diffusion coefficient.

1. Rise time and Duration Calculation

Calculating the rise time and duration of the blue flashes in the ASIM photometers uses the standard definition of rise time and duration. The rise time is defined as the time it takes for the event pulse to increase from 10% of the amplitude to 90% of the amplitude while the duration is defined as the rise time plus the time it takes for the event to subside from 90% of the amplitude to 10% of the amplitude. In practice, this is done by counting the number of samples within the interval defined above.

2. Parallax Correction

Satellite images of clouds far away from the local zenith will artificially displace cloud locations due to the viewing angle. Satellite images always assume the target is nadir which is not the case. To mitigate this error the parallax must be corrected by assuming an average cloud top height. Given the satellite height h, the radius of the earth r, the cloud height C_h and the event latitude l, one can generate a triangle which corrects for this parallax. The hypotenuse of this triangle by the law of cosines is:

$$d = \sqrt{(h+r)^2 + r^2 - 2R(h+r)\cos(l)} \tag{1}$$

Using this, we can find the angle, A of the triangle generated between the cloud and the ground as:

$$\phi = \sin^{-1}\left(\frac{(r+h)\sin(l)}{d}\right), A = \pi - \phi \tag{2}$$

and finally the length of the parallax p as

$$p = C_h \tan(A) \tag{3}$$

Once the length of the parallax is found, the event is moved length p on the surface of the Earth along the line between the satellite position and the event position.

3. Photon Intensity Derivation

Starting from equation 27 in (Luque et al., 2020) we have:

$$F(t) = \frac{\exp\left(-\frac{t}{\tau_A} - \frac{\tau_D}{t}\right)}{\sqrt{\pi}\tau_D}\left(\frac{t}{\tau_D}\right)^{-\frac{3}{2}} \tag{4}$$

where $\tau_D = \frac{L^2}{4D}$ and τ_A is the absorption. Introducing $\alpha = \frac{\tau_D}{t}$ and neglecting absorption we have

$$F(t) = F_\alpha(\alpha) = \frac{\exp\left(-\alpha\right)\alpha^{\frac{3}{2}}}{\sqrt{\pi}\tau_D} \tag{5}$$

The derivative is then:

$$F'_\alpha(\alpha) \;=\; \frac{1}{\sqrt{\pi}\tau_D}\exp\left(-\alpha\right)\left(-\alpha^{\frac{3}{2}} + \frac{3}{2}\sqrt{\alpha}\right) = \frac{\exp(-\alpha)\sqrt{\alpha}}{\sqrt{\pi}\tau_D}\left(\frac{3}{2} - \alpha\right). \tag{6}$$

The maximum is reached at $\alpha = \frac{3}{2}$ and is given by:

$$F_{max} = \frac{\exp\left(-\frac{3}{2}\right)\left(\frac{3}{2}\right)^{\frac{3}{2}}}{\sqrt{\pi}\tau_D} \tag{7}$$

And the flux can the be written in the original variable as

$$\frac{F(t)}{F_{max}} = \frac{\exp\left(\frac{3}{2} - \frac{\tau_D}{t}\right)}{\left(\frac{3}{2}\frac{t}{\tau_D}\right)^{\frac{3}{2}}} \tag{8}$$

which is equation 2 from the paper.

We note that it a function of only $\frac{t}{\tau_D}$ which makes it easy to solve for the rise time. 10% of the maximum is reached when $t_{10} = 0.171174\tau_D$ and 90% of the maximum is reached when $t_{90} = 0.468486\tau_D$ the 10% to 90% rise time is then $t_{90} - t_{10} = 0.297312$.

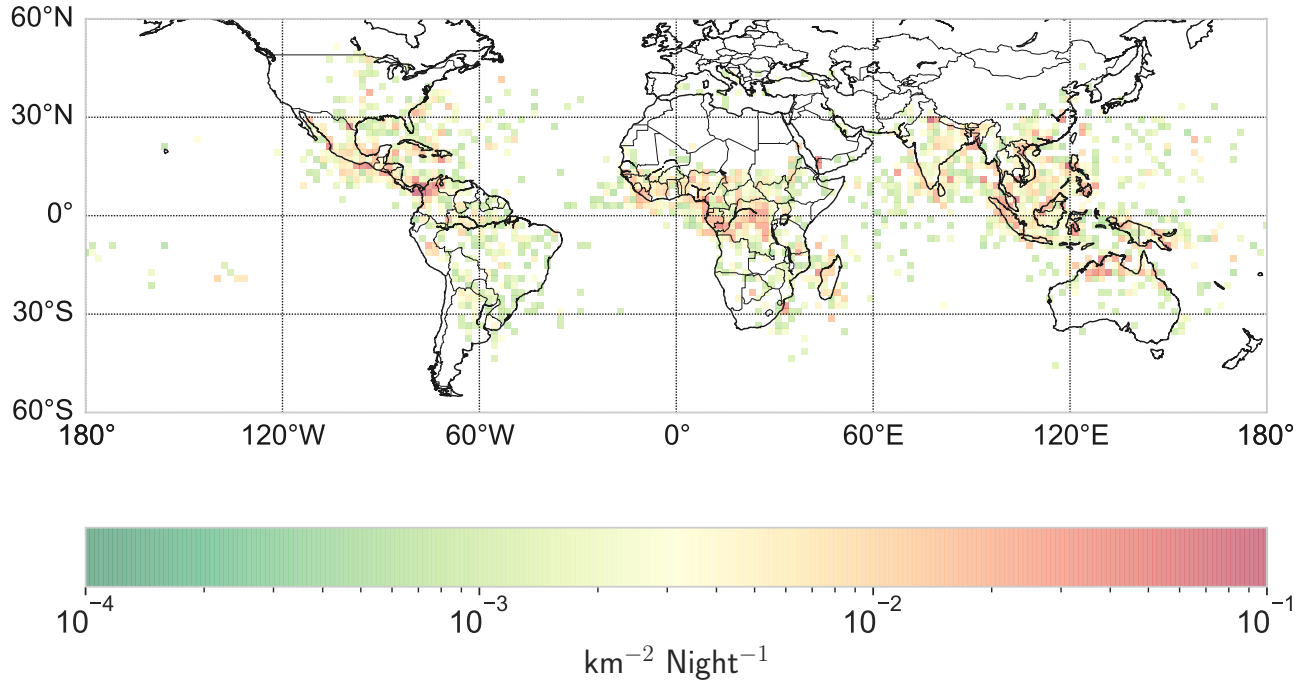

Figure S1. Non-smooth geographical distribution of BCD events with the same color scale as in the main paper with bins of size $2° \times 2°$.

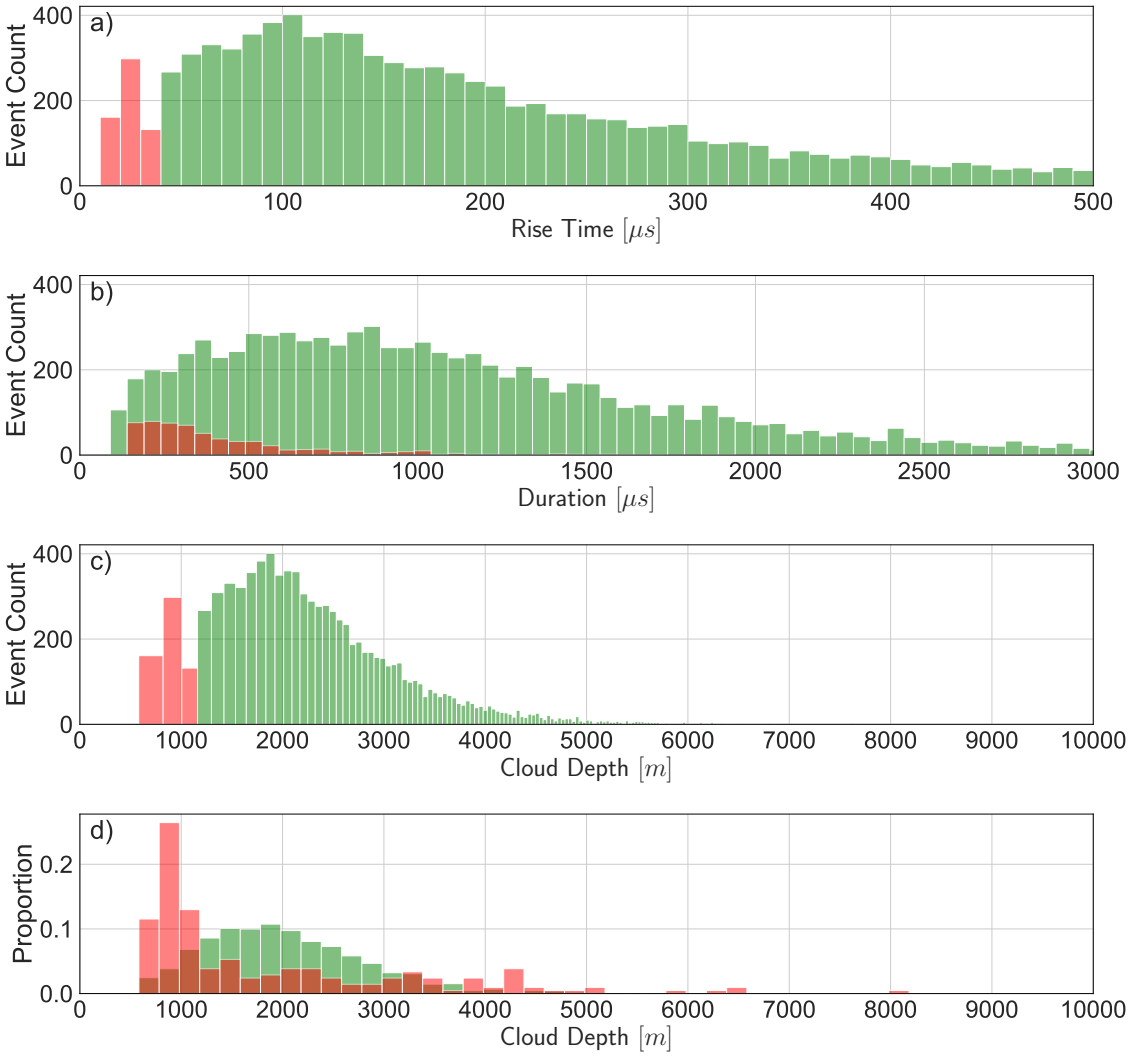

Figure S2. Recreation of figure 4 with $D = 2.5 \times 10^9 \mathrm{m}^2\mathrm{s}^{-1}$.